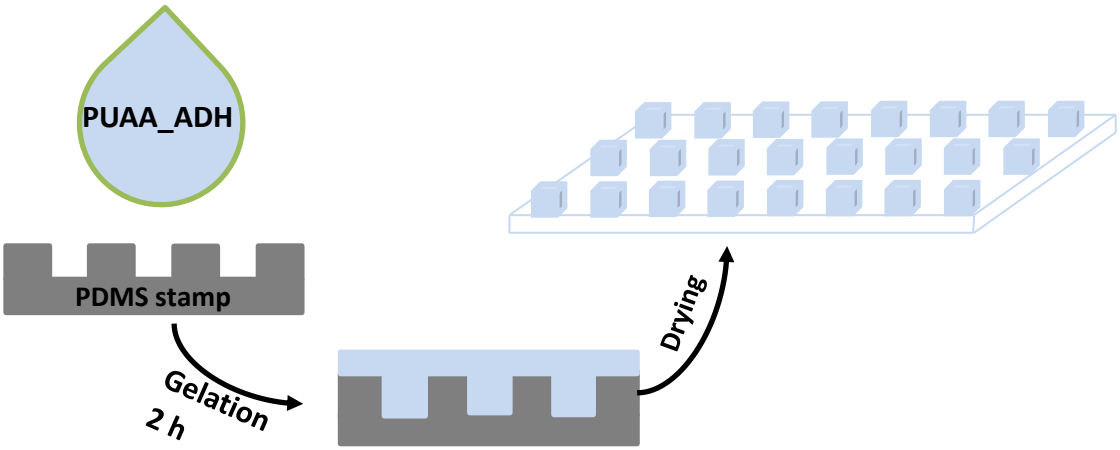

Figure S1. Schematic of the fabrication of patterned micro-cuboid PUAA-ADH hydrogel films.

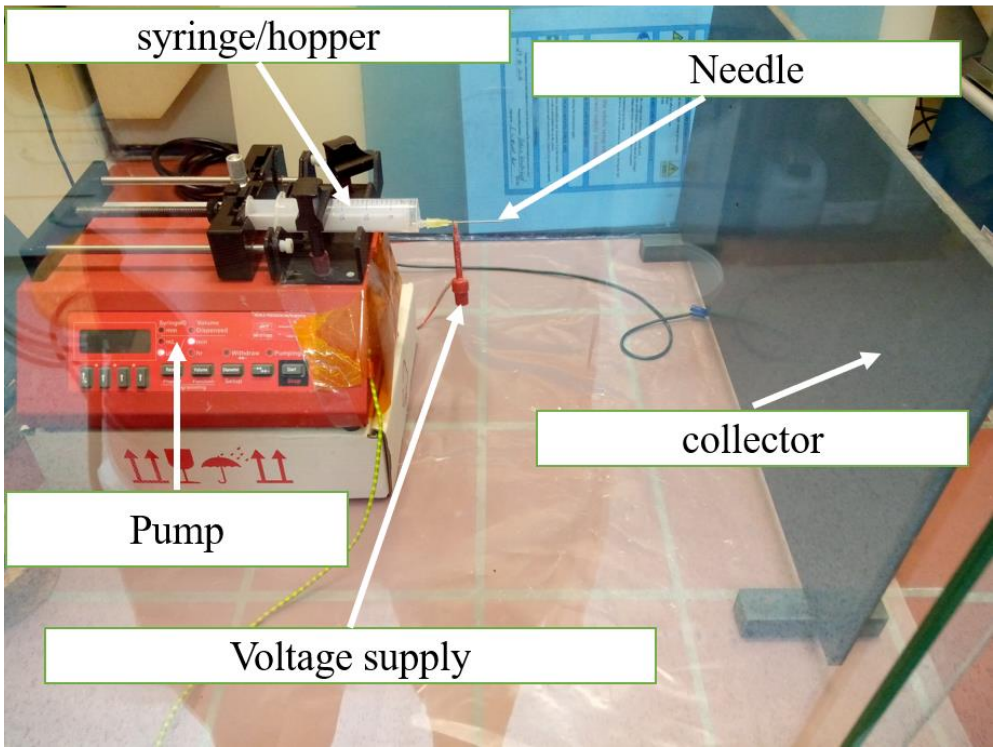

Figure S2. Electrospinning set-up used for producing chitosan-PEO electrospun nanofibers.

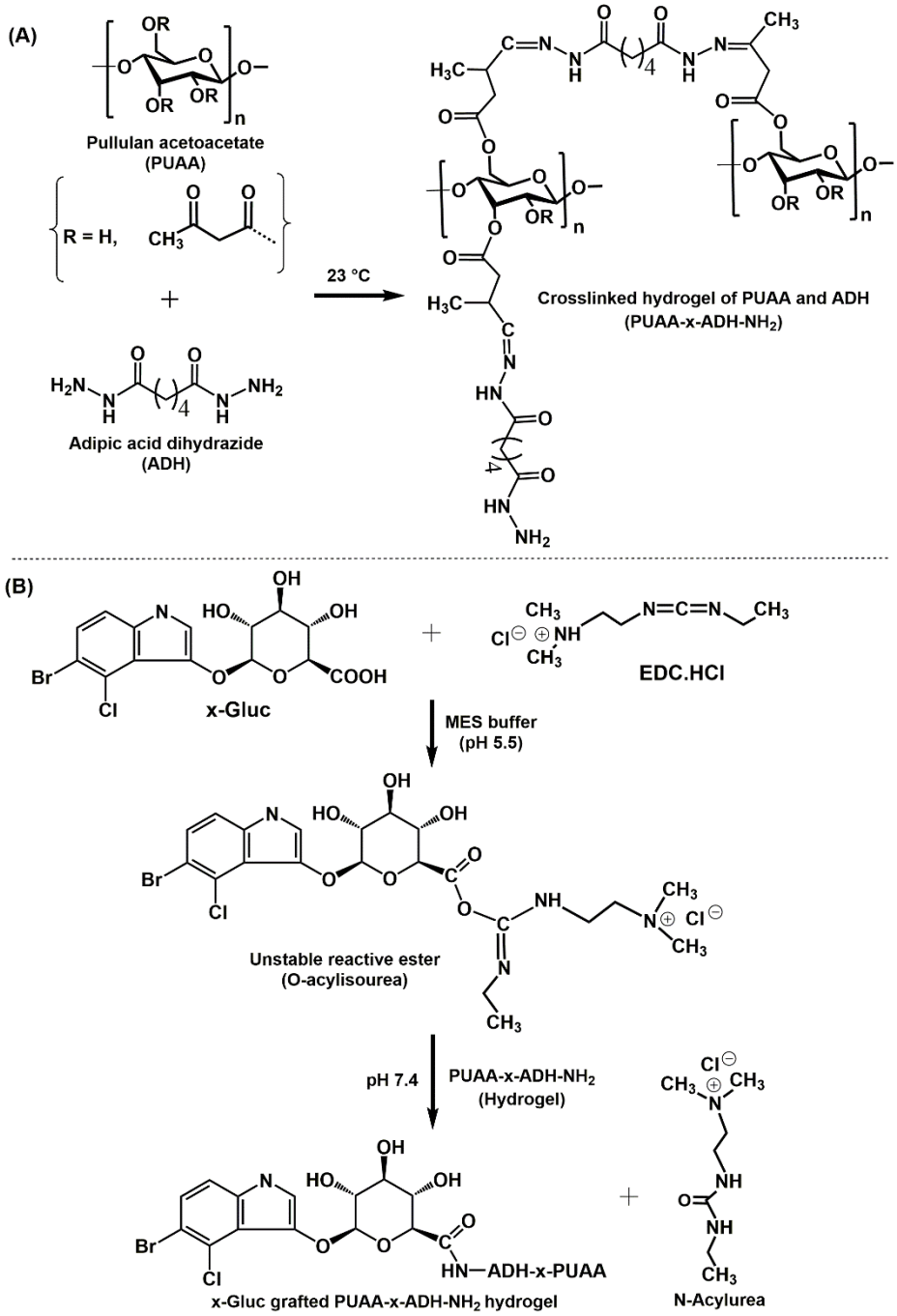

Figure S3. Schematic diagram of (A) the PUAA and ADH based crosslinked hydrogel, (B) modification of PUAA-ADH hydrogel through grafting of the chromogenic substrate (X-Gluc).

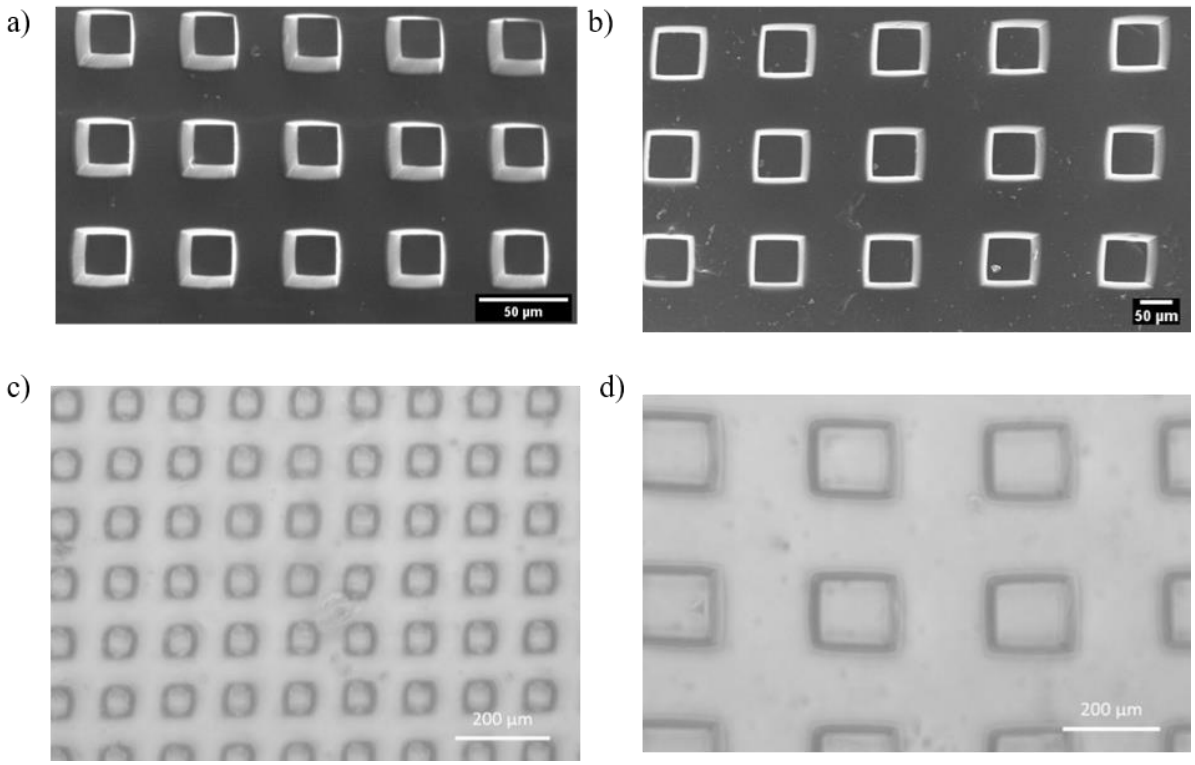

Figure S4. (a,b) Top view SEM images of the micro-cuboid structured hydrogel films after modifying with X-Gluc and drying under vacuum for 15 h. a) 40 µm film b) 100 µm film. (c, d) Optical microscopy images of the PUAA-ADH hydrogel films after swelling for 4 h c) 40 µm film d) 100 µm film.

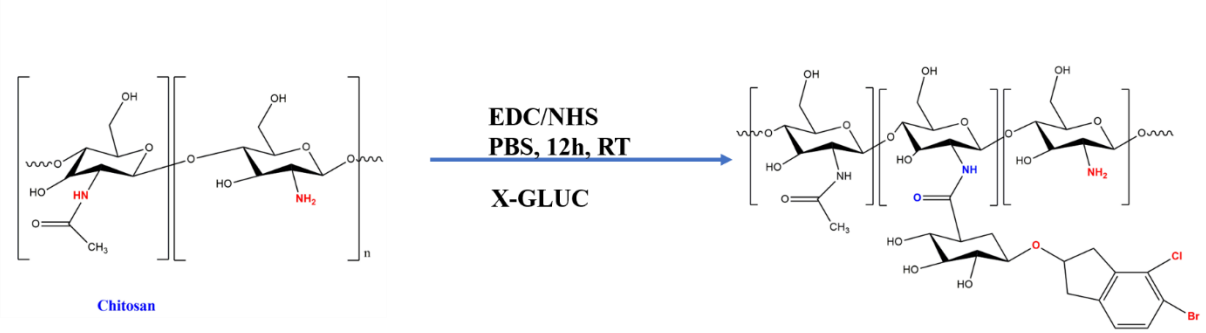

Chitosan

Chitosan grafted with X-Gluc

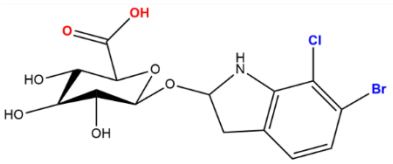

X-GLUC

5-Bromo-4-chloro-3-indoly-ß-D-glucuronide

Figure S5. Schematic of modification of chitosan with the chromogenic substrate X-Gluc.

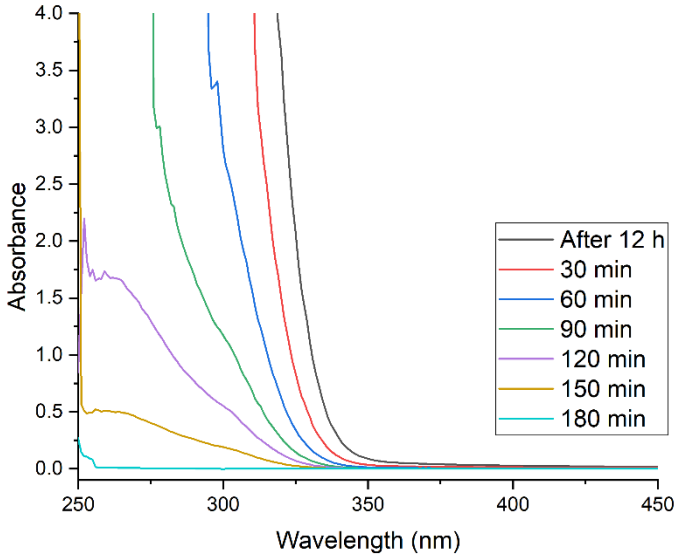

Figure S6. UV-Vis spectra of cleaning solution after modification of chitosan-PEO samples with chromogenic substrate X-Gluc.

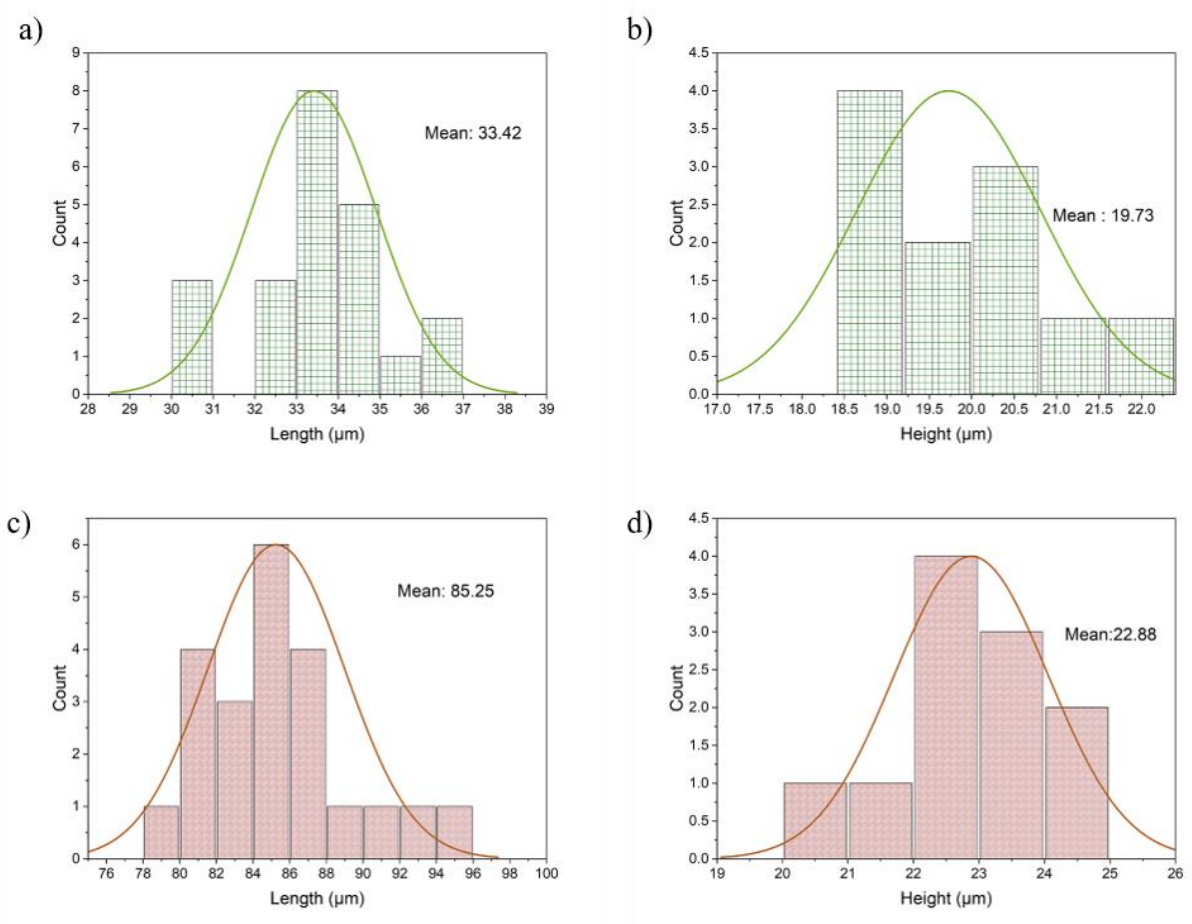

Figure S7. Length and height distribution of the hydrogel films fabricated using (a, b) a 40 μm template and (c, d) a 100 μm template.

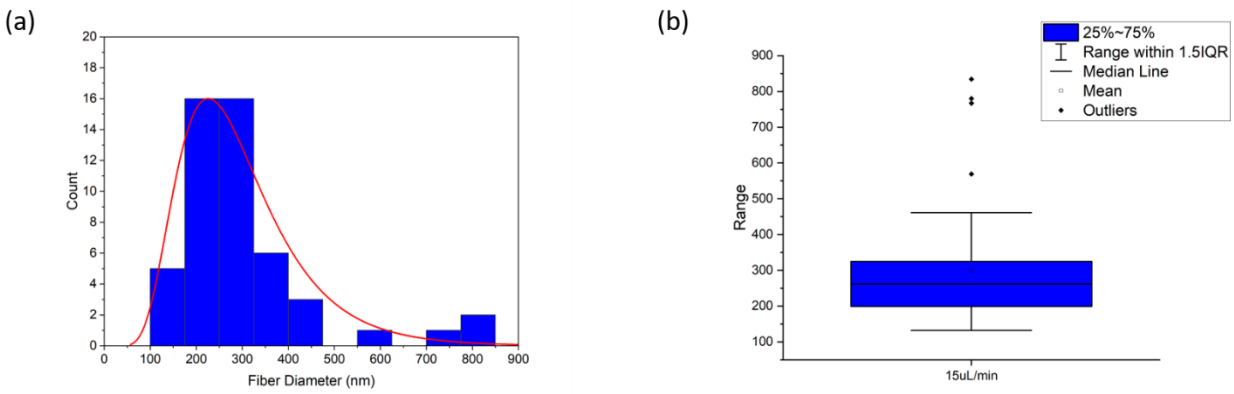

Figure S8. Sample histogram (a) and box and whisker plot (b) for a select electrospinning condition (15 µL/min, 20 kV & 15 cm). Outliers represent fibers not included in the calculation of the mean.

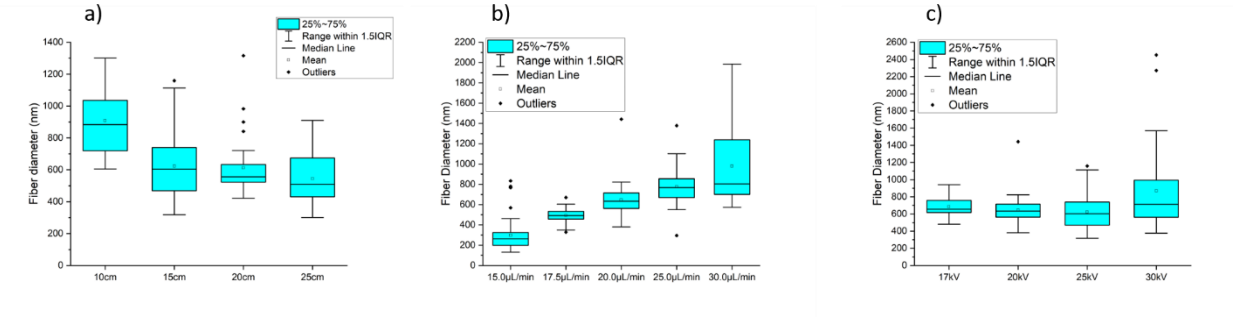

Figure S9. Box and whisker plots for mean fiber diameter for varied tip-to-collector distance (a), flow rate (b) and applied voltage (c).

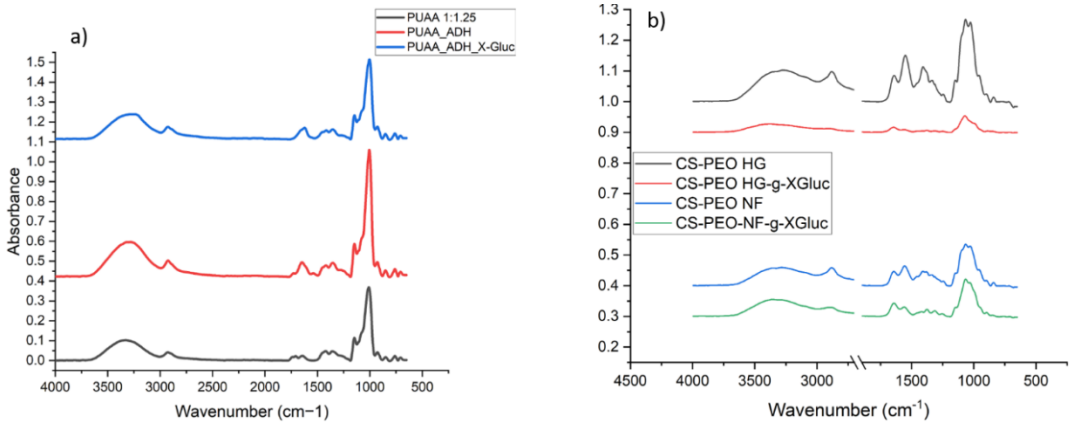

Figure S10. ATR-FTIR spectra of a) PUAA (1:125), PUAA_ADH and PUAA_ADH_X-Gluc, b) CS/PEO hydrogels and NFs and CS/PEO hydrogels and NFs with conjugated X-Gluc.

Table S1. Peak assignment for bands of interest observed in the FTIR spectra of CS/PEO NFs and hydrogels.

Assignment	Ref value range[1,2]	Unmodified		Modified	
		NF	Hydrogel	NF	Hydrogel
C-O-C	1070-1075	1067	1072	1068	1072
C-H	1375-1383	1375	1377	1375	1375
N-H (amide II)	1550-1565	1558	1548	1558	1544
NH_2	1590-1610	1591	1593	-	-
C=O (amide I)	1620-1655	1640	1643	1649	1644
O-H	3435-3455	3354	3340	3346	3350

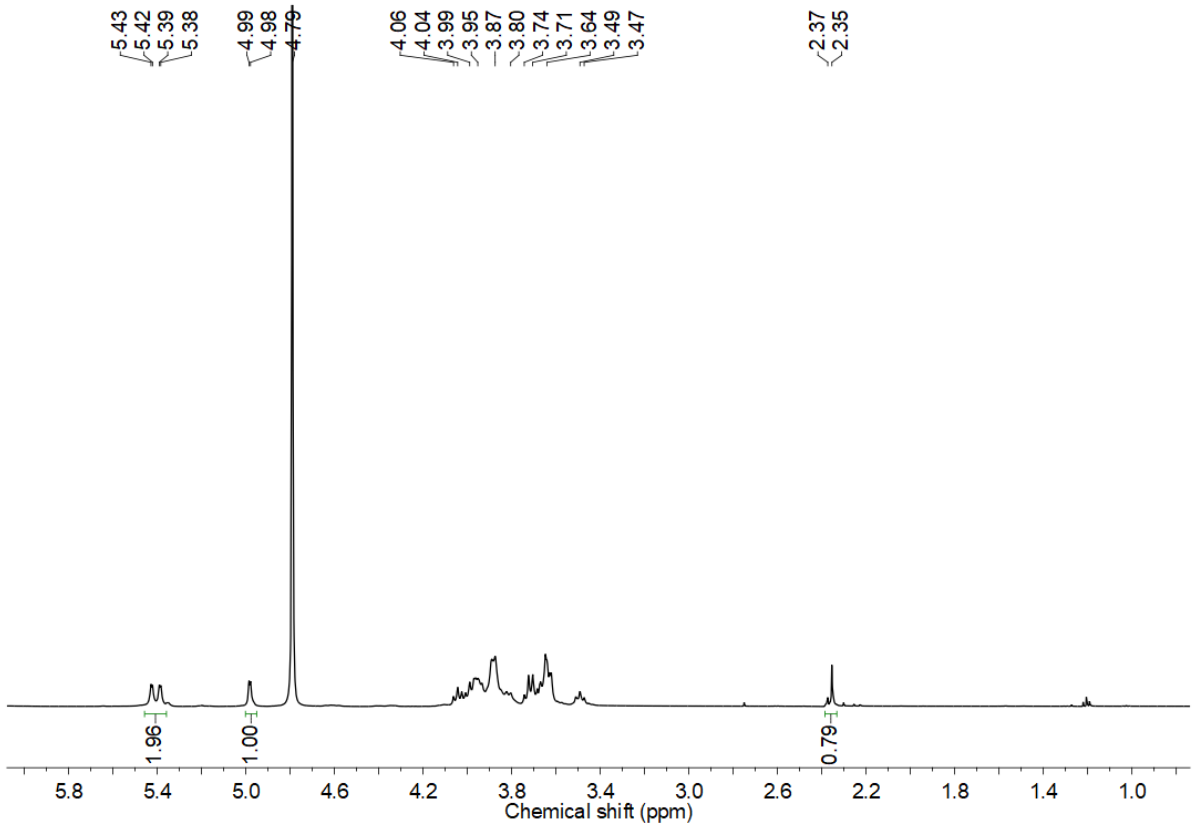

Figure S11. ^{1}H NMR spectrum of PUAA (1:1.25) measured in D_2O as solvent.

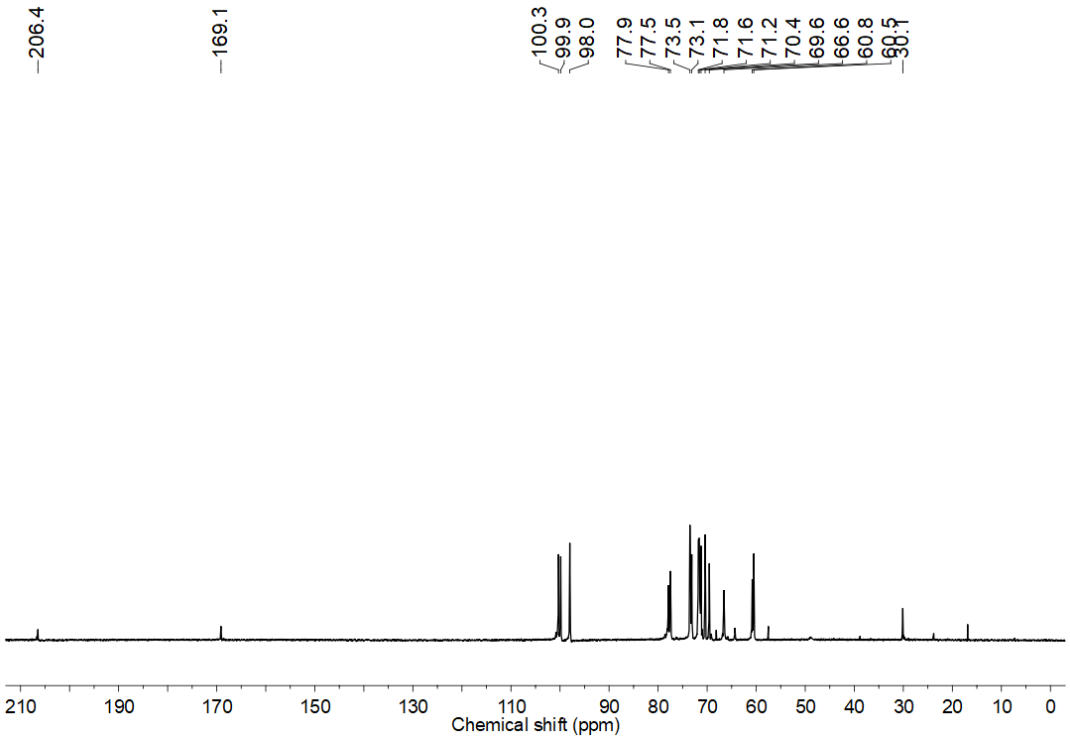

Figure S12. ^{13}C NMR spectrum of PUAA (1:1.25) in D_2O as solvent.

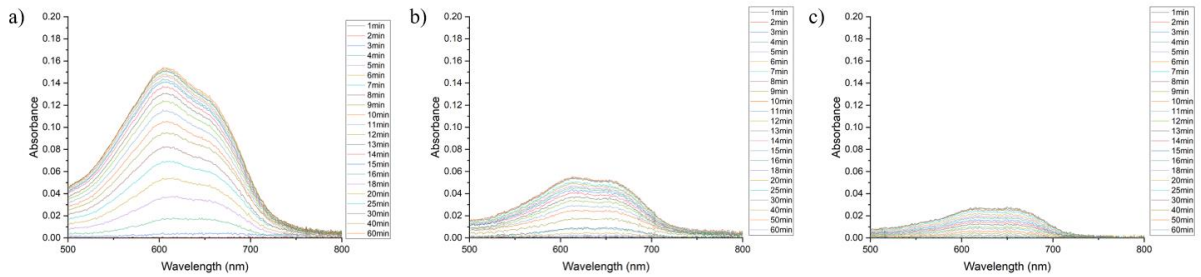

Figure S13. Absorbance spectra of varying substrate concentrations (a) 8 mg (b) 4 mg (c) 2 mg (40 µm, 50 nM fixed enzyme concentration).

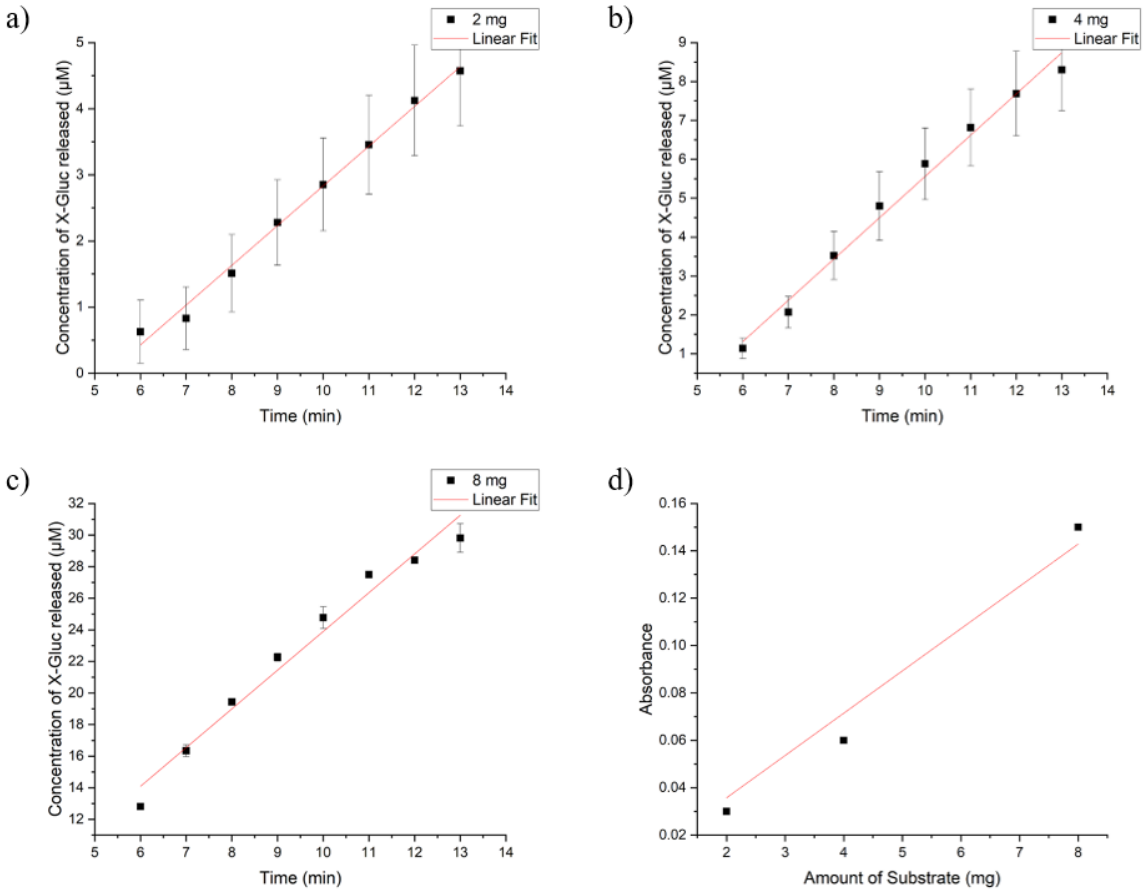

Figure S14. Linearly fitted plots of released X-Gluc concentration with time a) 2 mg, (b) 4 mg (c) 8 mg, (d) linearly fitted plot between absorbance and amount of substrate concentration (50 nM β-GUS) (error bars: standard error of the mean, n=3).

Table S2. Initial reaction rates of varying substrate concentration (i.e., 2 mg, 4 mg, 8 mg PUAA_ADH_X-Gluc films).

Enzyme concentration (nM)	Weight of dried Hydro-gel film (mg)	Rate of reaction (μM/min)	Adj. R^2
50	2.0	0.60	0.99
50	4.0	1.06	0.98
50	8.0	2.45	0.96

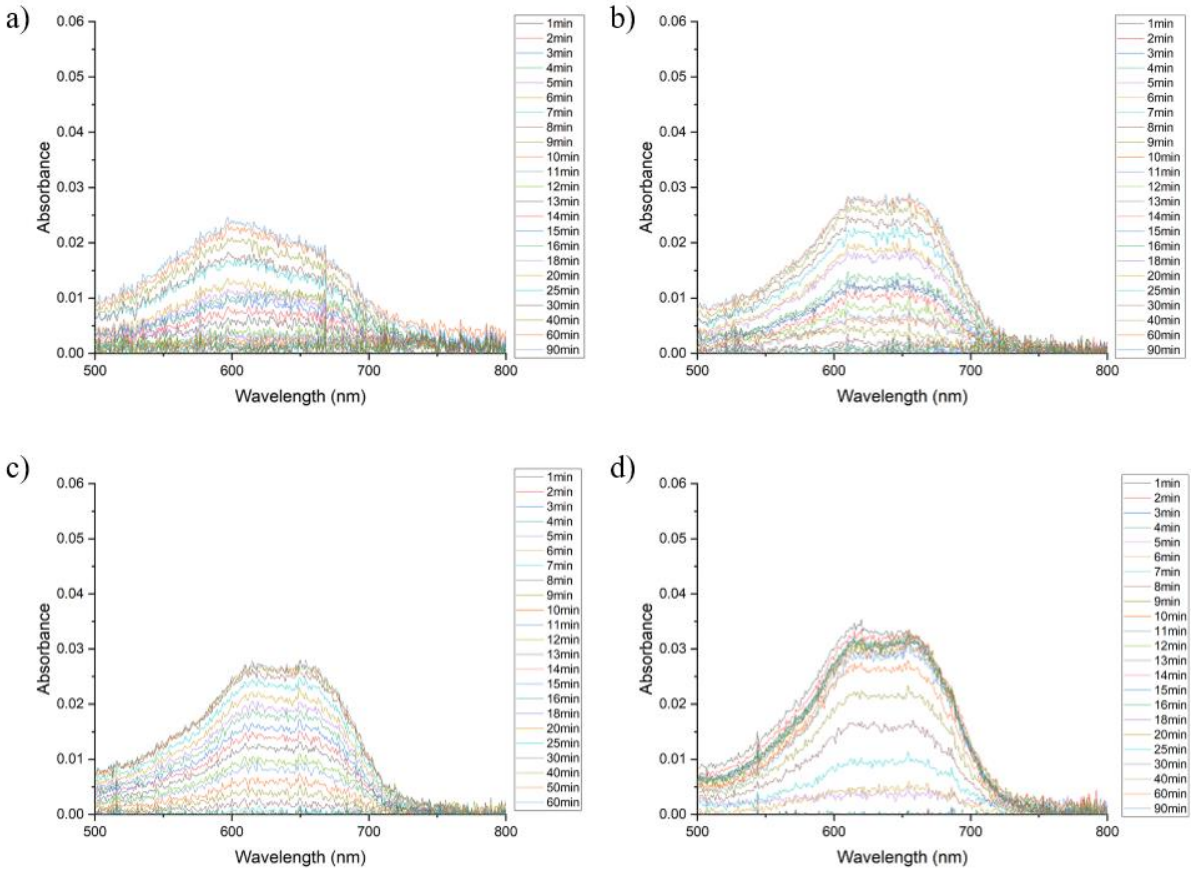

Figure S15. Absorbance spectra of varying enzyme concentrations (a) 25 nM (b) 35 nM (c) 50 nM (d) 100 nM β-GUS (40 μm, 2 mg patterned hydrogel film).

The initial apparent reaction rates were used to determine the V_{max} and K_m values according to the Lineweaver-Burk equation.

$$1/V_o = \left(K_m/V_{max}\right)\left(1/[s]\right) + \left(1/V_{max}\right)$$

Where the inverse of initial reaction rates was plotted against the inverse of the substrate concentration as in Figure S14.

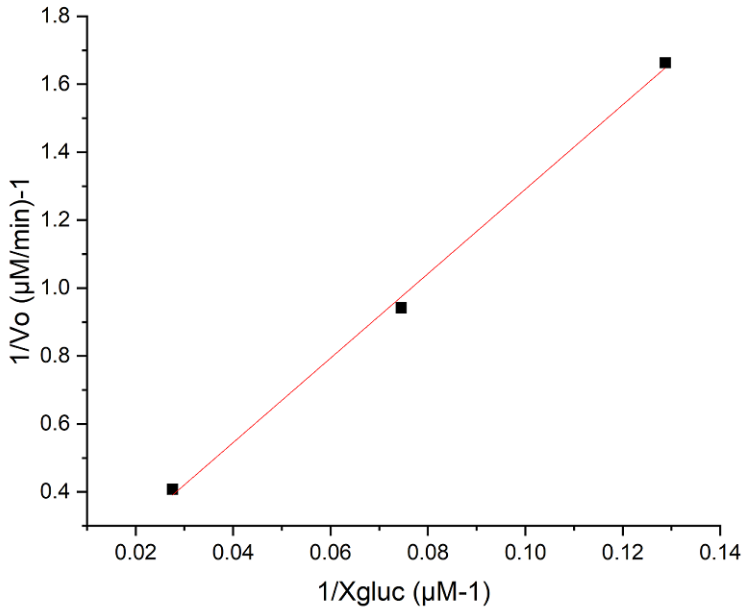

Figure S16. Linearly fitted graph between reciprocal of the initial reaction rate and reciprocal of the substrate concentration at a fixed β-GUS concentration (50 nM).

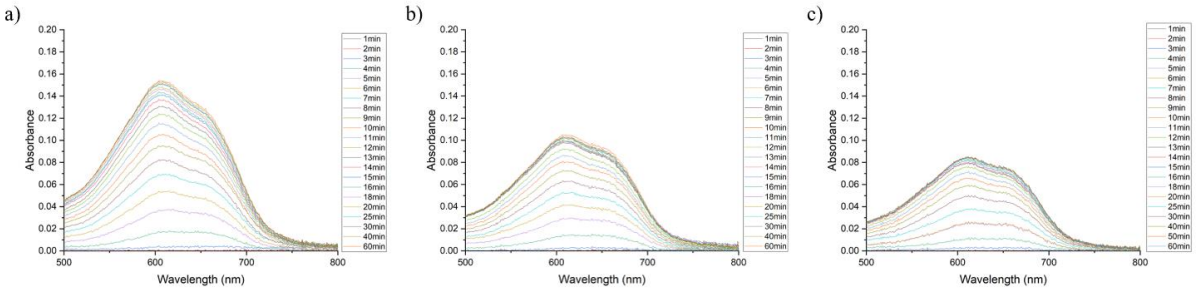

Figure S17. Absorbance spectra of varying surface area films (a) 40 µm (b) 100 µm (c) control film (bulk non-structured film, 50 nM fixed enzyme concentration).

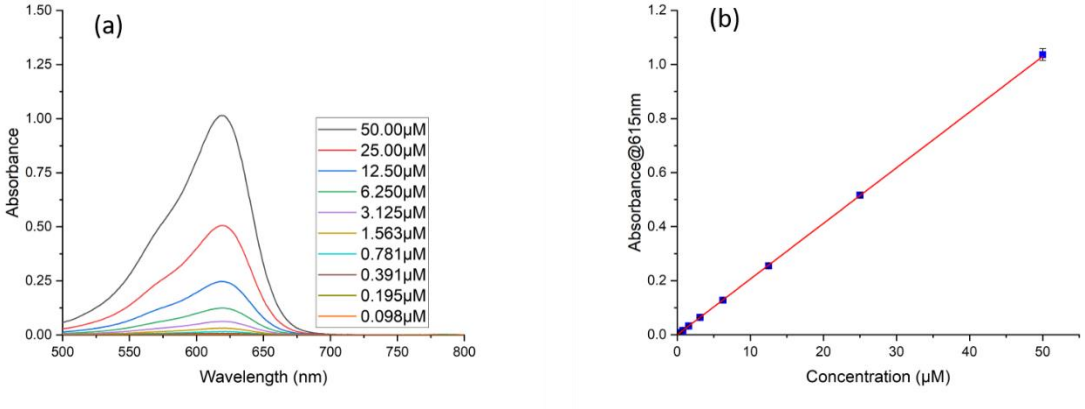

Figure S18. Calibration curve. (a) UV-Vis absorbance spectra of indigo. (b) Maximum absorbance peak at λ_{max}=615nm (standard deviation, error bars for n=3, R^2=0.99968).

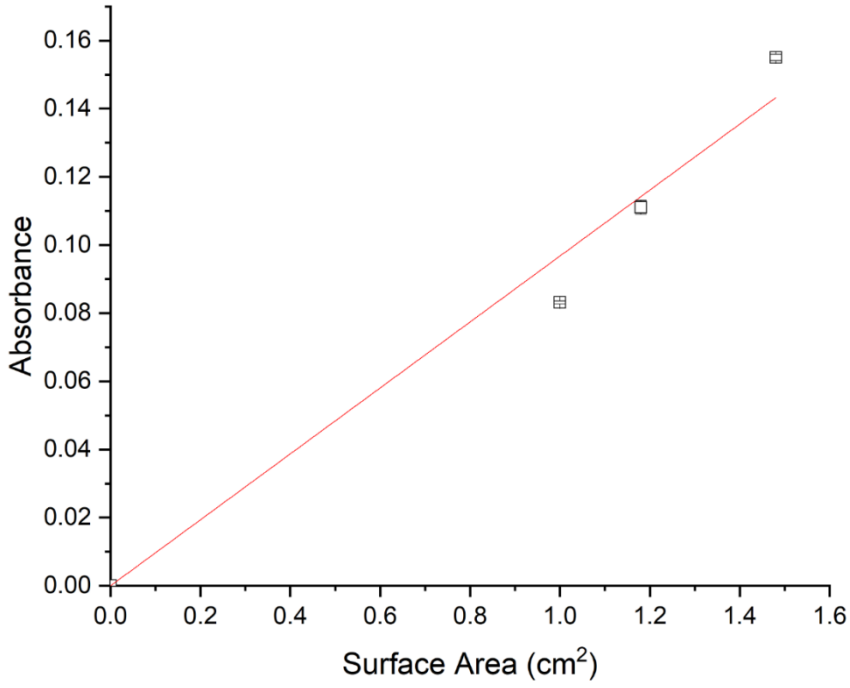

Figure S19. Relation between absorbance and surface area of PUAA-ADH-X-Gluc hydrogel films at (fixed β-GUS concentration 50 nM).

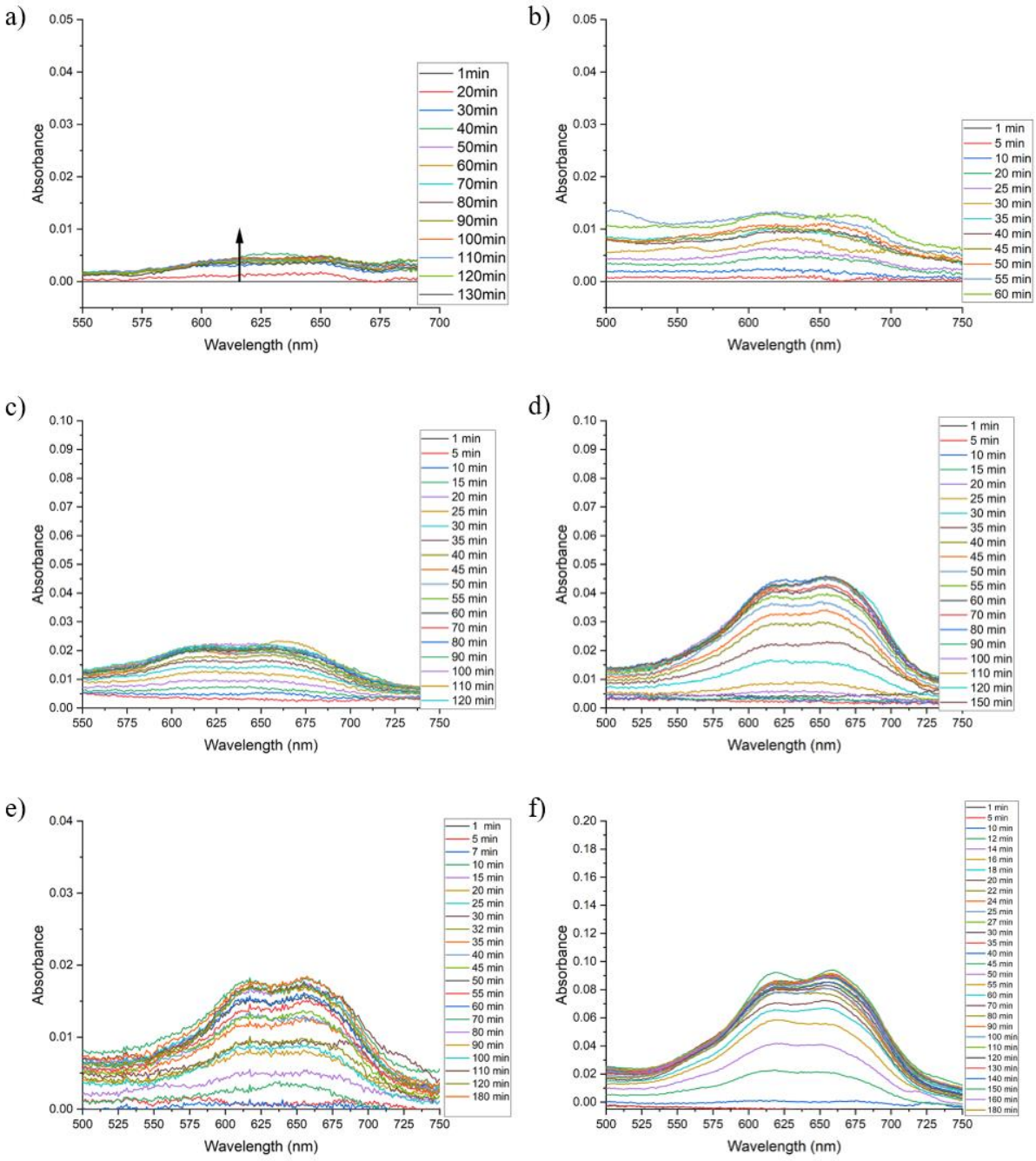

Figure S20. UV-vis spectra from enzymatic hydrolysis reactions. (a) 2 mg hydrogel, (b) 2 mg NFs, (c) 3 mg hydrogel, (d) 3 mg NFs, (e) 4 mg hydrogel and (f) 4 mg NFs.

Table S3. Initial reaction rates of varying substrate concentration (i.e., 2 mg, 3 mg, 4 mg) for X-Gluc modified chitosan- PEO nanofibers and hydrogel.

Substrate amount	Apparent reaction rate

(mg)	NFs		Hydrogel	
	× 10^{-4}	R^2	x10^{-4}	R^2
2	2.47	0.991	0.85	0.972
3	5.92	0.991	4.35	0.983
4	8.27	0.996	8.05	0.978

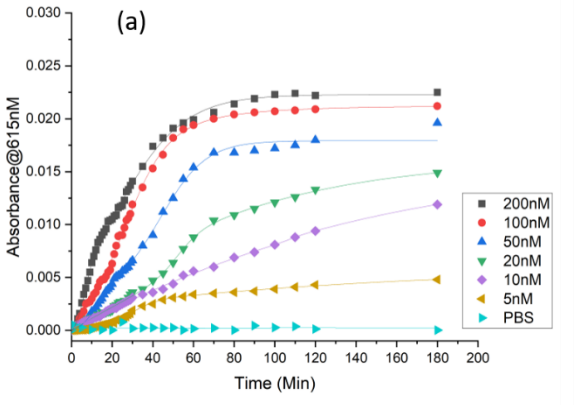

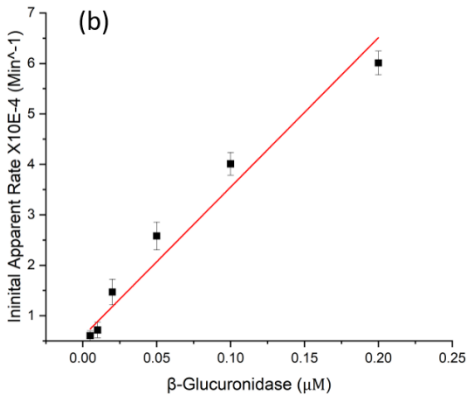

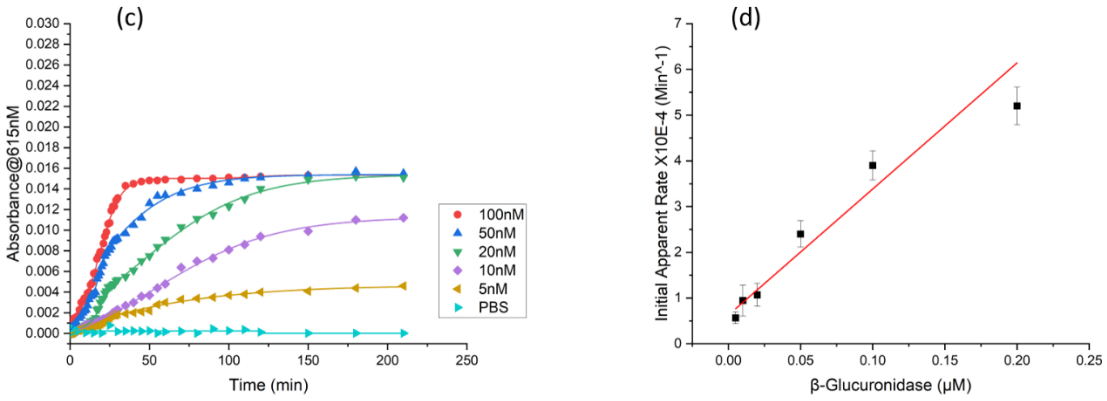

Figure S21. Kinetics recorded as absorbance at λ_{max} = 615 nm for the β-glucuronidase sensing using (a) NFs and (c) hydrogel and estimated initial apparent rate of reaction for the first minutes from linear least-squares fit for (b) NFs and (d) hydrogel (error bars: standard error of mean for n=2, R^2=0.969 for NFs and 0.940 for CS/PEO HG).

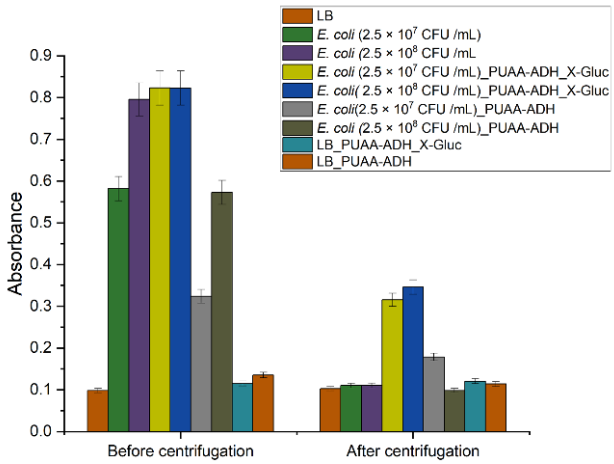

Figure S22. Absorbance at λ_{max} = 615 nm of the wells in Figure 12(b and c) before and after centrifugation at 4 °C for 10 min at 7500 rpm.

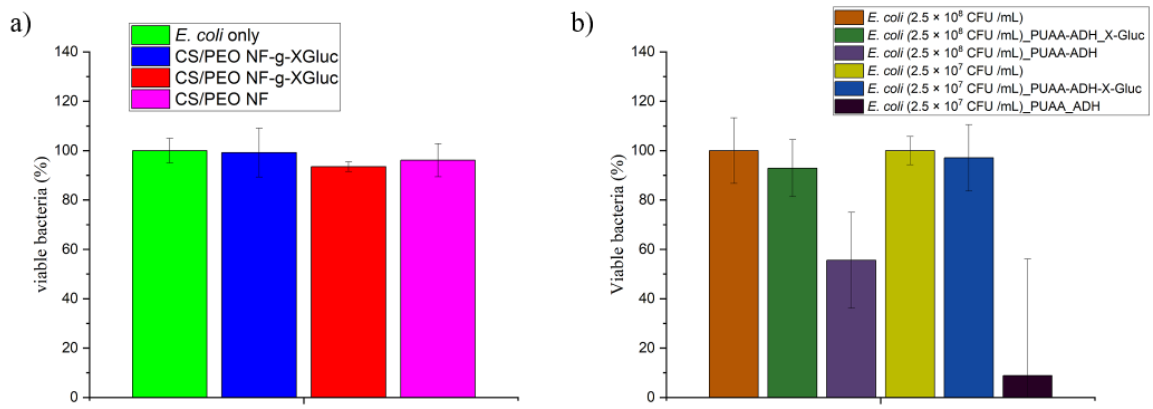

Figure S23. Fraction of viable bacteria (determined by CFU/ mL counting) in presence of a) modified CS/PEO NFs compared to untreated *E. Coli* suspension (CFU/mL=2.36×10^7). b) PUAA-ADH_X-Gluc film, and PUAA-ADH film, compared to untreated to *E. coli* control suspension (starting concentration; 2.5×10^8 CFU /mL, and 2.5×10^7 CFU /mL) after 20 h incubation. (Error bars show maximal deviation between duplicate counts).

References

[1] Ebrahimi, M.M.S.; Voss, Y.; Schönherr, H. Rapid Detection of Escherichia coli via Enzymatically Triggered Reactions in Self-Reporting Chitosan Hydrogels. *ACS Appl. Mater. Interfaces* **2015**, *7*, 20190-20199.

[2] Kasaai, M.R. A Review of Several Reported Procedures to Determine the Degree of N-Acetylation for Chitin and Chitosan Using Infrared Spectroscopy. *Carbohydr. Polym.* **2008**, *71*, 497-508